Electronic Supplementary Material

A 3D Porous WP_2 nanosheets@carbon cloth flexible electrode for efficient electrocatalytic hydrogen evolution

Mingyu Pi [1], Xiaodeng Wang[1], Dingke Zhang[2], Shuxia Wang[1], Shijian Chen (✉)[1]

1 College of Physics, Chongqing University, Chongqing 401331, China

2 College of Physics and Electronic Engineering, Chongqing Normal University, Chongqing 401331, China

E-mail: sjchen@cqu.edu.cn

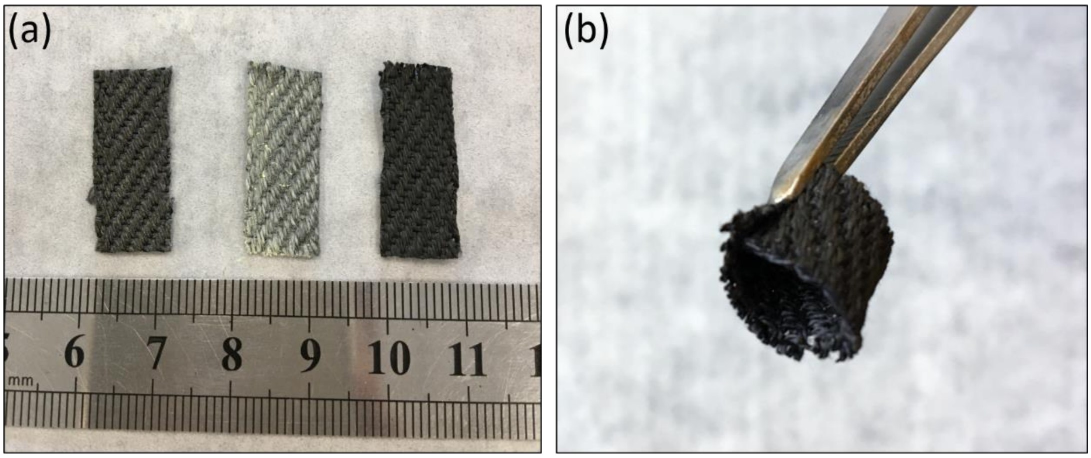

Fig. S1 (a) Photographs of bare CC, WO_3 NSs/CC and WP_2 NSs/CC; (b) Photograph of the fabricated flexible WP_2 NSs/CC electrode

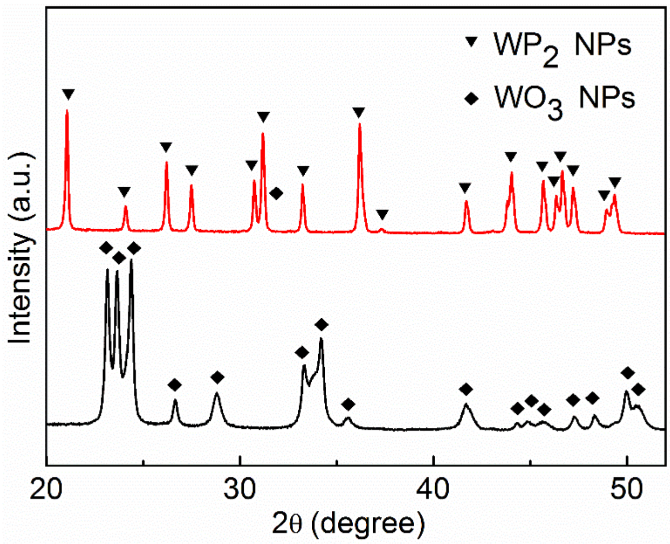

Fig. S2 XRD patterns for WO_3 and WP_2 nanoparticles

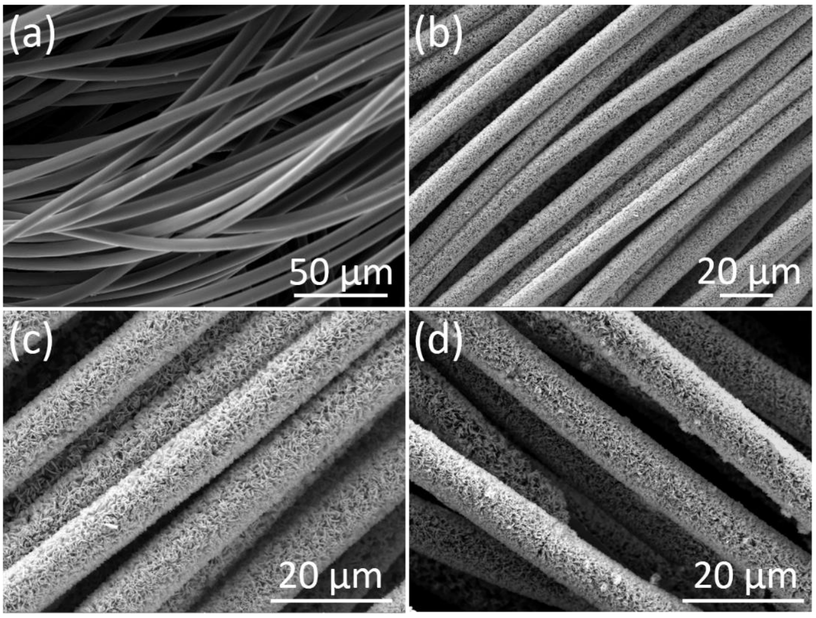

Fig. S3 Low-magnification SEM images for (a) blank CC substrate, (b, c) WO_3 NSs/CC and (d) WP_2 NSs/CC

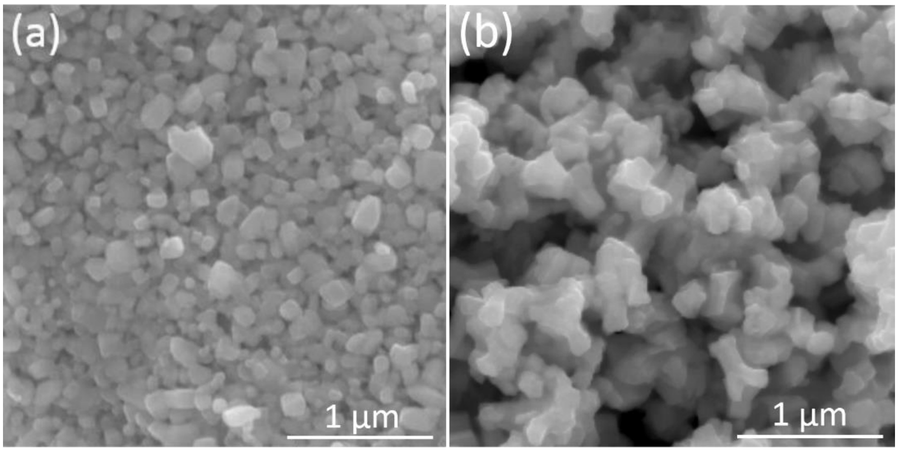

Fig. S4 SEM images of (a) WO_3 and (b) WP_2 nanoparticles

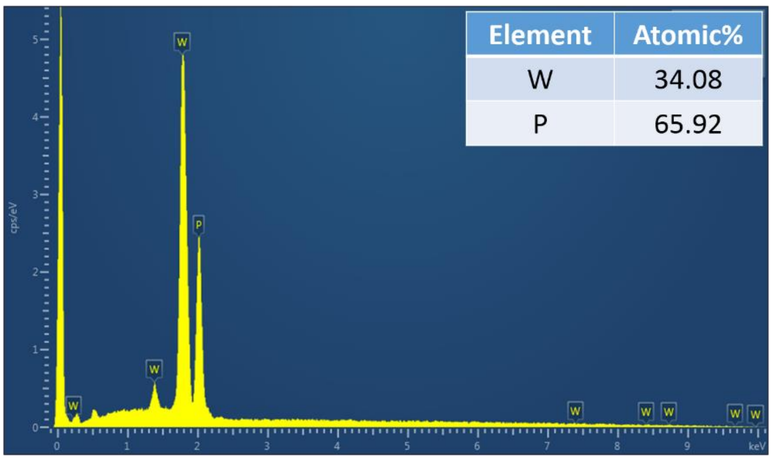

Fig. S5 EDX spectrum for WP_2 NSs

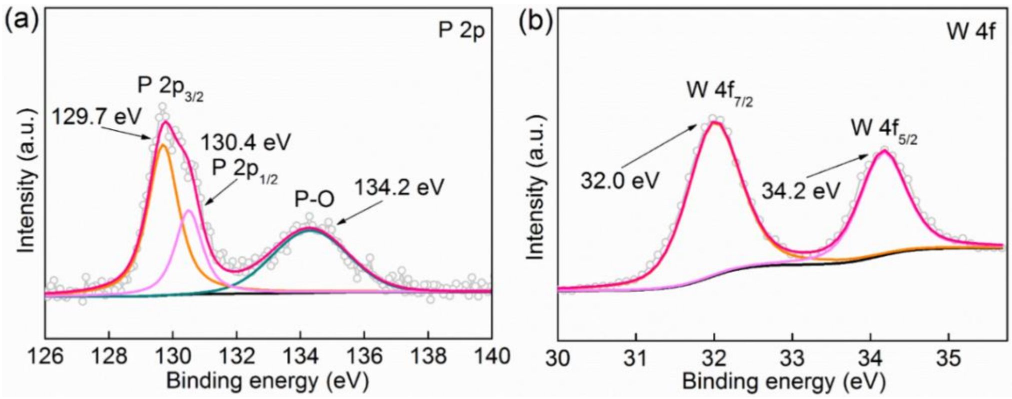

Fig. S6 XPS spectra in (a) P and (b) W regions for WP_2 NSs/CC

Table S1 Comparison of HER performance of in acidic media of WP_2 NSs/CC with other non-noble metal electrocatalsts (NWs: nanowires, NRs: nanorods, NSs: nanosheets, NPs: nanoparticles and SPs: submicron particles)

Catalyst	Current density/ (mA·cm^{-2})	Corresponding overpotential/ mV	Reference
WP_2 NSs/CC	10	135	This work
W_2C	10	~140	J. Mater. Chem. A, 2016, 4: 8204–8210
WN NRs/CC	10	198	Electrochim. Acta., 2015, 154: 345–351
WS_2	10	310	Chem. Commun., 2015, 51: 8334–8337
WP_2 NPs	10	143	Energy Technol., 2016, 4: 1030–1034
WP_2 SPs	10	201	Electrochim. Acta, 2016, 216: 304–311
WP_2 NRs	10	~200	Energy Environ. Sci., 2016, 9: 1468–1475
WP_2 SPs	10	161	ACS Catal., 2015, 5: 145–149
WP_2 NRs	10	148	J. Power Sources, 2015, 278: 540–545
WP NRs/CC	10	130	ACS Appl. Mater. Interfaces, 2014, 6: 21874–21879
MoP_2 NPs/Mo	10	143	Nanoscale, 2016, 8: 8500–8504
MoP NSs/CF	10	200	Appl. Catal. B: Environ., 2015, 164: 144–150
MoP/NC	10	~130	Electrochim. Acta., 2016, 199: 99–107
MoP-CA2	10	125	Adv. Mater., 2014, 26: 5702–5707
FeP_2/C	10	＞500	J. Mater. Chem. A, 2015, 3: 499–503
FeP NSs	10	＞200	Chem. Commun., 2013, 49: 6656–6658
Cu_3P NW/CF	10	143	Angew. Chem. Int. Ed., 2014, 53: 9577–9581
CoP NPs	10	~150	Electrochim. Acta., 2016, 199: 99–107
CoP/CNT	10	122	Angew. Chem. Int. Ed., 2014, 53: 3710–6714
$Ni_{12}P_5$/NC	10	~230	Electrochim. Acta., 2016, 199: 99–107

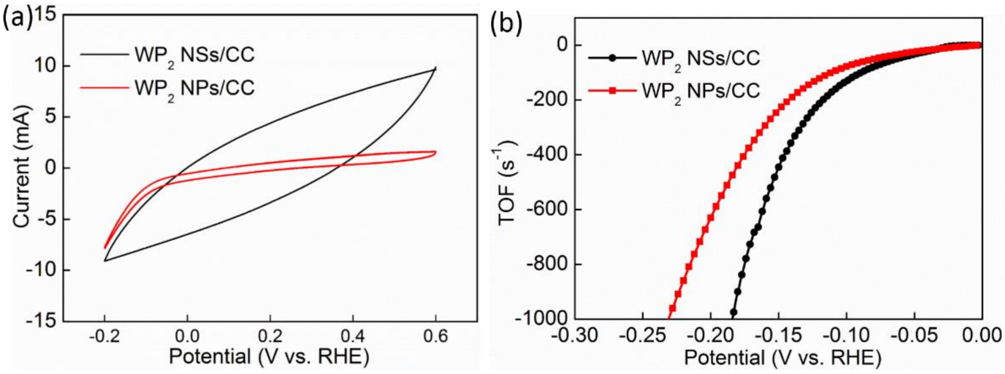

Fig. S7 (a) CVs for WP_2 NSs/CC and WP_2 NPs/CC in phosphate (pH=7) over a range of –0.2 to 0.6 V at a scan rate of 50 mV·s^{-1} and (b) TOFs for WP_2 NSs/CC and WP_2 NPs/CC

The number of active sites (n) was examined via cyclic voltammograms in phosphate buffer (pH = 7) at a scan rate of 50 mV·s^{-1} between –0.2 V and +0.6 V vs. RHE and n (mol) could be determined with the following equation:

$$n = Q/2F$$

Where Q (C) is the voltammetric charge, F is Faraday constant (96480 C·mol^{-1}). For WP_2 NSs/CC, Q is 3.39×10^{-2} C, n is 3.51×10^{-7} mol. For WP_2 NPs/CC, Q is 1.63×10^{-2} C, n is 1.68×10^{-7} mol. TOF (s^{-1}) could be calculated with the following equation:

$$TOF = I/2nF$$

Where I (A) was the current of the polarization curve obtained by LSV measurements.

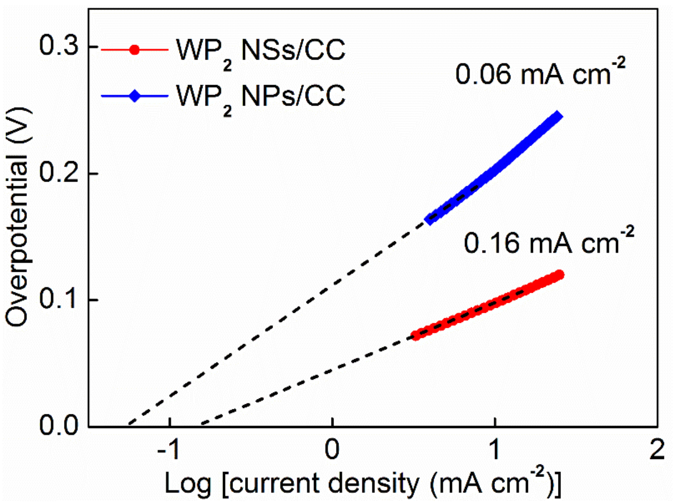

Fig. S8 Calculated exchange current density for WP_2 NSs/CC and WP_2 NPs/CC in 0.5 mol·L^{-1} H_2SO_4 by applying extrapolation method to the Tafel plot

Table S2 Comparison of exchange current density of WP_2 NSs/CC with other non-noble metal electrocatalsts (NWs: nanowires, NRs: nanorods, NSs: nanosheets, NPs: nanoparticles and SPs: submicron particles)

Catalyst	Exchange current density/(mA·cm^{-2})	Reference
WP_2 NSs/CC	0.16	This work
MoS_2/FTO	6.9×10^{-4}	Nat. Mater., 2012, 11: 963–969
defect-rich MoS_2	8.9×10^{-3}	Adv. Mater., 2013, 25: 5807–5813
MoO_3-MoS_2/FTO	8.2×10^{-5}	Nano Lett., 2011, 11: 4168–4175
bulk Mo_2C	1.3×10^{-3}	Angew. Chem. Int. Ed., 2012, 51: 12703–12706
bulk MoB	1.4×10^{-3}	Angew. Chem. Int. Ed., 2012, 51: 12703–12706
Co-NRCNTs	0.01	Angew. Chem. Int. Ed., 2014, 126: 4372–4376
WS_2 NSs	0.02	Nat. Mater., 2013, 12: 850–855
$CoSe_2$ NP/CP	$(4.9\pm1.4)\times10^{-3}$	J. Am. Chem. Soc., 2014, 136: 4897–4900
Ni_2P hollow NPs	0.033	J. Am. Chem. Soc., 2013, 135: 9267–9270
Cu_3P NW/CF	0.18	Angew. Chem. Int. Ed., 2014, 53: 9577–9581
FeP_2/C	1.75×10^{-3}	J. Mater. Chem. A, 2015, 3: 499–503
CoP NWs/CC	0.288	J. Am. Chem. Soc., 2014, 136: 7587–7590
CoP/CNT	0.13	Angew. Chem. Int. Ed., 2014, 53: 3710–6714
WP NRs/CC	0.29	ACS Appl. Mater. Interfaces, 2014, 6: 21874–21879
WP_2 NPs	0.09	Energy Technol., 2016, 4: 1030–1034
WP_2 SPs	0.017	ACS Catal., 2015, 5: 145–149
WP_2 NRs	0.013	J. Power Sources, 2015, 278: 540–545
bulk MoP	0.034	Energy Environ. Sci., 2014, 7: 2624–2629
MoP-CA2	0.086	Adv. Mater., 2014, 26: 5702–5707
MoP_2 NS/CC	0.83	J. Mater. Chem. A, 2016, 4: 7169–7173
MoP_2 NPs/Mo	0.06	Nanoscale, 2016, 8: 8500–8504

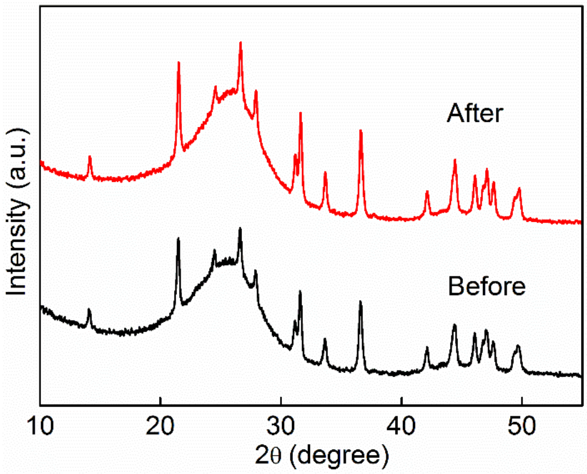

Fig. S9 XRD patterns before and after reaction for WP_2 NSs/CC

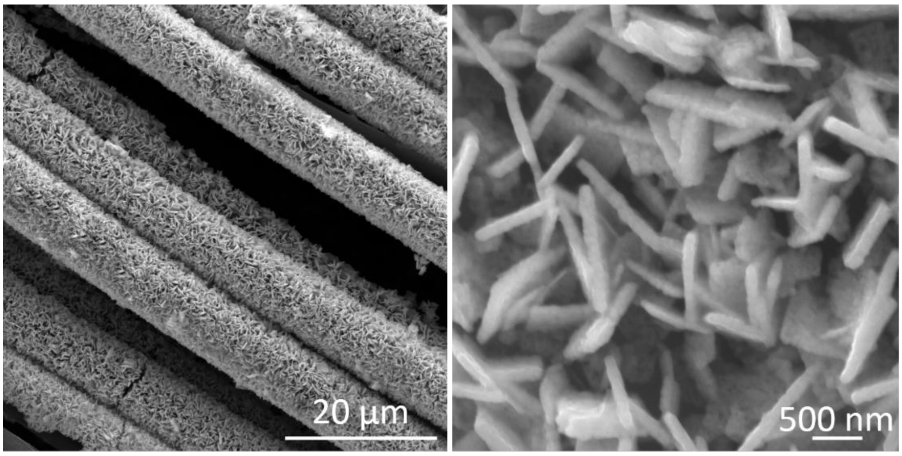

Fig. S10 SEM images for WP_2 NSs/CC after the electrochemical tests

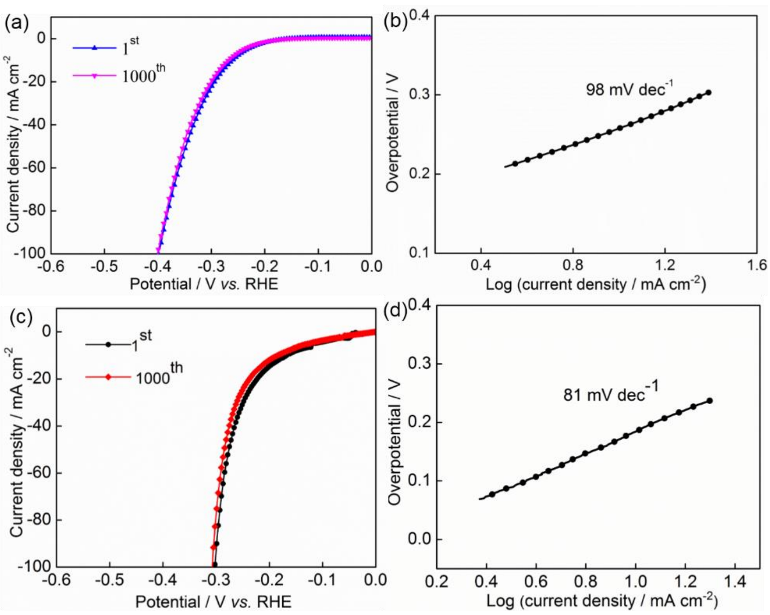

Fig. S11 Polarization curves for the WP_2 NSs/CC in (a) 1.0 M PBS (pH=7) and (c) 1.0 M KOH (pH=14); (b, d) Corresponding Tafel plots

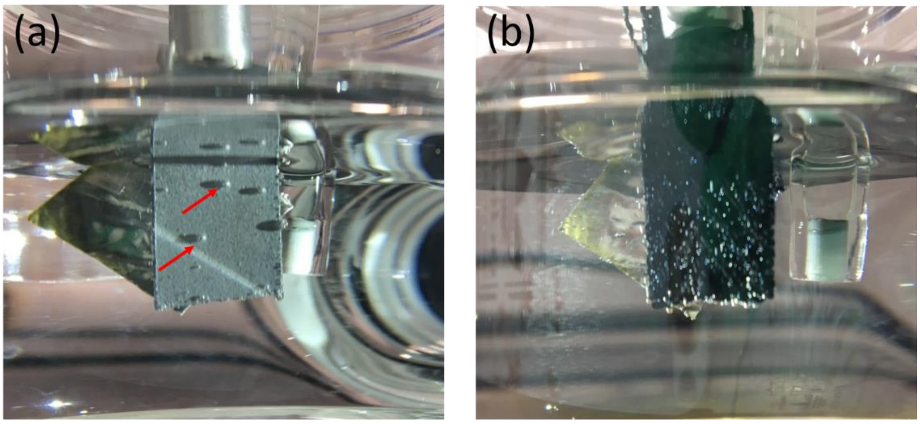

Fig. S12 Digital photographs of operating WP_2 film and nanosheet (NS) array electrodes evolving H_2. (a) For WP_2 film electrodes, large H_2 bubbles commonly pin at the electrode surface, as red arrows marked; (b) Due to the NS morphology, many small H_2 bubbles rapidly form at and escape from the WP_2 NS electrode surface

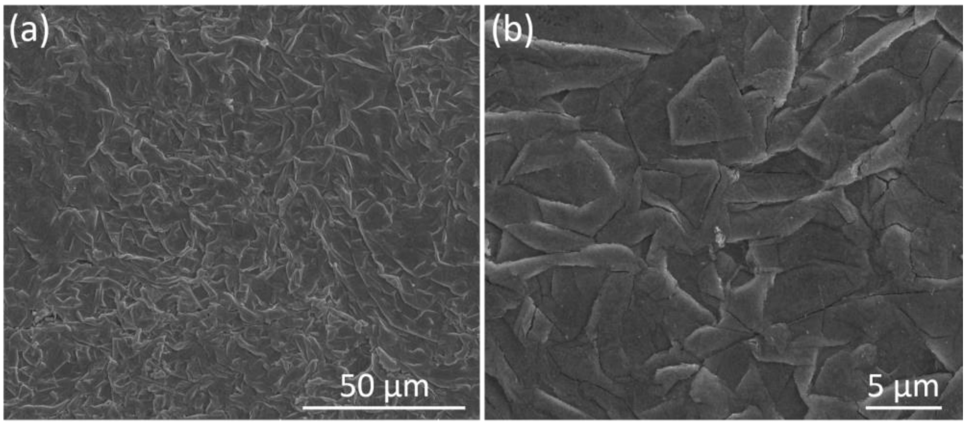

Fig. S13 SEM images for WP_2 film catalyst

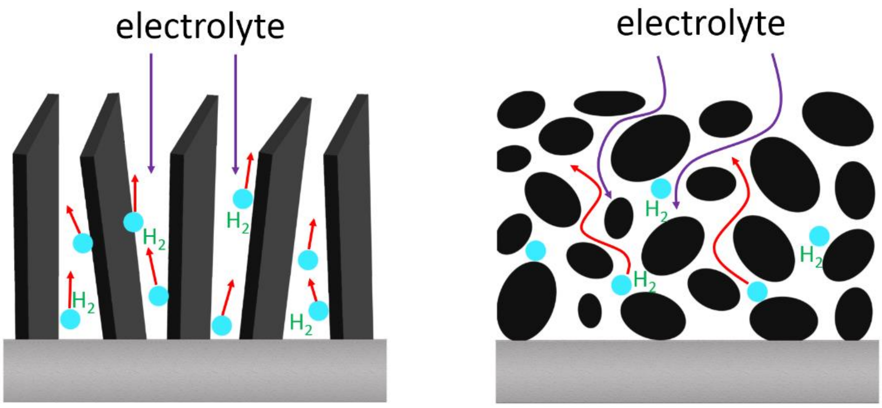

Fig. S14 Schematic depictions of the nanosheets structure of the catalyst can provide smooth hydrogen evolution channels, thus allowing fast removal of the H_2 bubbles from the electrode surface and avoid the peeling of the catalysts, which display a large structural advantage compared to the conventional electrode with drop coated catalyst

Table S3 Comparison of energy barrier for hydrogen atom adsorption and bond length for WP_2 catalyst with the other catalysts

Catalyst	Energy barrier for transition state of hydrogen atom adsorption/eV	Bond length/Å	Reference
WP_2	0.92	1.45	This work
Pt	0.67	-	
MoP	1.05	1.42	J. Power Sources, 2016, 328: 551
MoP_2	0.93	1.44	
Pt	0.67	-	
$MoS_2/CoSe_2$	1.13	-	Nat. Commun., 2015, 6: 5982
Pt	0.69	-	J. Am. Chem. Soc., 2015, 137: 1587
Co-FeS_2/CNT	1. 23	1.365	
FeS_2/CNT	1. 62	1.361	